Theory of stochastic resonance

Bruce McNamara* and Kurt Wiesenfeld
School of Physics, Georgia Institute of Technology, Atlanta, Georgia 30332
(Received 19 October 1988)

The concept of *stochastic resonance* has been introduced previously to describe a curious phenomenon in bistable systems subject to both periodic and random forcing: an *increase* in the input noise can result in an *improvement* in the output signal-to-noise ratio. In this paper we present a detailed theoretical and numerical study of stochastic resonance, based on a rate equation approach. The main result is an equation for the output signal-to-noise ratio as a function of the rate at which noise induces hopping between the two states. The manner in which the input noise strength determines this hopping rate depends on the precise nature of the bistable system. For this reason, the theory is applied to two classes of bistable systems, the double-well (continuous) system and the two-state (discrete) system. The theory is tested in detail against digital simulations.

I. INTRODUCTION

The original work on stochastic resonance by Benzi *et al.*, in which the term was coined, was in the context of modeling the switching of the Earth's climate between ice ages and periods of relative warmth with a period of about 100 000 years.[1-3] The eccentricity of the Earth's orbit varies with that period, but according to current theories the variation is not strong enough to cause such a dramatic climate change. By introducing a bistable "climatic potential" they suggested that a cooperative phenomenon between the weak periodic variation in the eccentricity (the "signal") and the other random fluctuations might account for the strong periodicity observed. While calling this mechanism stochastic resonance, they correctly pointed out that this is not strictly a resonance in the sense of an increased response when a driving frequency is tuned to a "natural frequency" of the system. There is, however, a useful analogy to resonance in that the signal-to-noise ratio (the "response") is maximized when some parameter—in this case the input noise—is tuned near a certain value.

The essential ingredients for stochastic resonance consist of a bistable system, with two inputs—a coherent signal and random noise—and with an output which is some function of the inputs and the internal dynamics of the system. For the moment we may view the system as a "black box" and look at how the output power changes as the input signal and noise are varied. For a system well characterized by linear-response theory (that is, with linear or "mildly" nonlinear internal dynamics) the signal-to-noise ratio (SNR) at the output must equal the SNR at the input, and any increase in the input noise will result in a decrease in the output SNR. In contrast, the signature of stochastic resonance is an *increase* in the output SNR with increased input noise. Thus the nonlinear nature of the problem is crucial.

In fact, the first papers on stochastic resonance focused on the behavior of the signal output and not the SNR. However, this focus has subsequently shifted: It is more interesting both theoretically and experimentally to define stochastic resonance in terms of the SNR.

Of the two experimental papers that have reported observation of stochastic resonance, one involved a Schmitt trigger electronic circuit[4] and the other a bidirectional ring laser.[5] The Schmitt trigger circuit is particularly interesting because it is nicely modeled as a discrete two-state system with hysteresis. Though it is not obvious how to compare the results to the two-well theories,[1-3,6] the basic phenomenon was clearly demonstrated. The authors also report that "the noise is almost suppressed" when the output at the signal frequency is most enhanced.[4] We interpret this to mean they observed a dramatic example of a secondary effect predicted by the theory of Sec. III: Power fed into the signal is balanced by an equal amount of power subtracted from the noise output integrated over all frequencies.

The other existing experiment used a bidirectional ring laser,[5] which can be made to switch between clockwise and counterclockwise modes like the switching of an overdamped particle in a double-well potential.[7] With a signal and noise input affecting the laser's preference for one or the other mode, the output light intensity was shown to have a signal-to-noise ratio displaying stochastic resonance, as shown in Fig. 1. The theory presented below was briefly sketched there. Though the effect was clearly demonstrated experimentally, there were too many free parameters in fitting the data to provide a convincing check on the theory.

A complete theory of stochastic resonance should address several issues. Ideally one would like to have an expression for the output power spectrum as a function of all of the system's parameters. In particular, expressions for the output signal amplitude S and noise level N would allow one to find the value of input noise for which the SNR is a maximum, and the important dependence on the signal frequency ω_s could be studied. Also important is the matter of generality—what are the essential features common to all systems which can show stochastic resonance, and can the theory be applied to a wide variety of such systems? Especially useful would be a theory which divides cleanly into a generic part, depend-

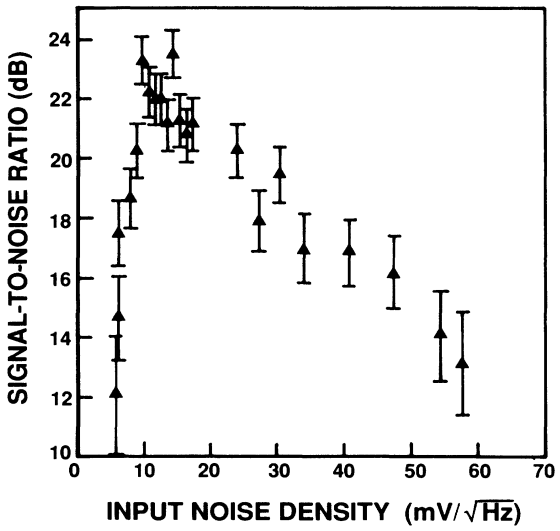

FIG. 1. Signal-to-noise ratio as a function of input noise from the ring laser system of Ref. 5.

ing only on the broad features of all such systems, and a part which depends on the particulars of the system being studied.

In order to put the present work in context, we turn to a brief review of the literature on this topic. In the papers by Benzi *et al.*[1-3] and the paper by Nicolis,[6] the emphasis was on understanding a particular problem: the mechanism behind the large, nearly periodic variations in the Earth's climate. These papers have in common a Kramers rate approach to hopping between a warm well and a cold well of a one-dimensional climatic potential. Using a heuristic argument they propose a loose range of input noise variance D within which the effect is predicted to take place and show suggestive simulation data to support their claim. The range of D proposed corresponds to the location of the maximum value for S, not SNR, in the low-frequency regime. These arguments hinge on the relative sizes of the two relevant time scales in the problem, namely, the hopping time and the modulation period. Eckmann and Thomas focused on two issues not addressed before.[8] One was to analyze a somewhat simpler two-state system in which the dynamical variable may only take on one of two discrete values, $x = \pm c$. For reasons addressed in Sec. VI, the two-state system has important differences from the double well which make the effect of varying the input noise D more difficult to analyze. Eckmann and Thomas also emphasized the effect of varying the signal frequency, with D held fixed.

In a later work, the same basic approach of Benzi *et al.* was applied to the real-valued Landau-Ginzburg equation.[9] This seems to be the only attempt thus far to look for stochastic resonance in a spatially extended system. No attempt is made here to study such systems.

In a very recent work, Fox has studied the problem of stochastic resonance using an eigenfunction approach.[10] The strength of this approach rests in its generality, generating a formal expression for the power spectrum for an arbitrary one-dimensional potential. However, to determine whether stochastic resonance is present requires evaluation of specific eigenfunctions and eigenvalues for the particular problem at hand, which can only be done analytically in rare instances. The formal perturbation expansions have been evaluated for a specific potential, namely, the "double square well",[10,11] and the resulting features reproduce the basic phenomenon quite well. Fox and co-workers have also discussed stochastic resonance in a nonhysteretic, two-state switch.[12]

Finally, though not specifically concerned with stochastic resonance, there are other relevant works which discuss periodically and stochastically forced bistable systems. Among these, Caroli *et al.*[13] use an adiabatic eigenfunction expansion to study the periodically modulated double well. This may be viewed as an alternative approach to the less formal derivation presented in Sec. III for the evolution of the probability density for the bistable system to lie somewhere in one of the two states. Finally, Bryant *et al.*[14] derive the signal and noise *gains* for a particle in a modulated quartic potential, that is, the ratio of the output signal to the input signal power and the output noise to the input noise. However, in this work the effect of varying D was not studied.

The goal of the present work is to provide a detailed study of stochastic resonance, including a comparison of theory with digital simulations. We present results for both continuous and discrete systems, and the expressions for S and N allow detailed examination of the effects of both D and ω_s, as well as any other parameters of interest. Despite the difference in definition, the earlier double-well results[1-3] agree with our general rate equation approach, when the latter is applied to the low-frequency regime.

Throughout, we emphasize the relationship between the theoretical results and the experimental determination of the relevant quantities. We stress that there is some subtlety involved: For example, the choice of bandwidth in determining the output power can greatly affect the numerical value of the signal-to-noise ratio (though not the existence of stochastic resonance) as the noise strength is varied.

The central feature of the theory for stochastic resonance developed below is a rate equation relating the change in the probability $n_+(t)$ of a particle being in one of the two states to the rates at which particles flow into and out of that state. The rate equation is a simple first-order differential equation, but to write down an expression for its solution in general requires using a Taylor expansion for the transition rates $W_\pm(t)$. Having solved for the probability $n_+(t)$, it is a straightforward matter to derive the power spectrum of the discrete-state variable x. This much of the analysis is sufficiently general to be applicable to a wide range of bistable systems driven by signal and noise. However, the precise expression for $W_\pm(t)$ will depend on the particular system under study, and stochastic resonance is not manifest in the equations without this.

We begin the body of this paper with a more detailed background of the phenomenon. In Sec. III we derive approximate expressions for the output signal and noise power in the general manner described above. A careful

discussion concerning the subtleties involved in comparing the theoretical results with real experiments and digital simulations is presented in Sec. IV. In Sec. V we apply the theory to continuous, double-well systems using a Kramers theory to relate the input noise to the transition time between wells. In addition, comparison is made with digital simulations and with the results of Benzi *et al.* Two-state systems are addressed in Sec. VI, with the Schmitt trigger problem used as an example. Again a comparison is made with digital simulations. Section VII provides a brief summary and conclusions.

II. BACKGROUND

A physical picture of stochastic resonance must emphasize the essentially nonlinear nature of the dynamics of the system. To fix ideas, consider the bistable double-well potential of Fig. 2(a) subject to no noise and no periodic forcing. A heavily damped particle will come to rest at one of the two minima of the potential, which are located at $\pm c$. In the presence of a moderate amount of random forcing, it is well known that the particle will still spend *most* of its time near $\pm c$, but will make occasional transitions over the barrier in the center. As the input noise variance, D, is increased, the rate at which such jumps will occur, W, increases. Typically, W grows very rapidly with D at first, but once D is large enough that the barrier becomes relatively easy to surmount, W grows more slowly as D is further increased.

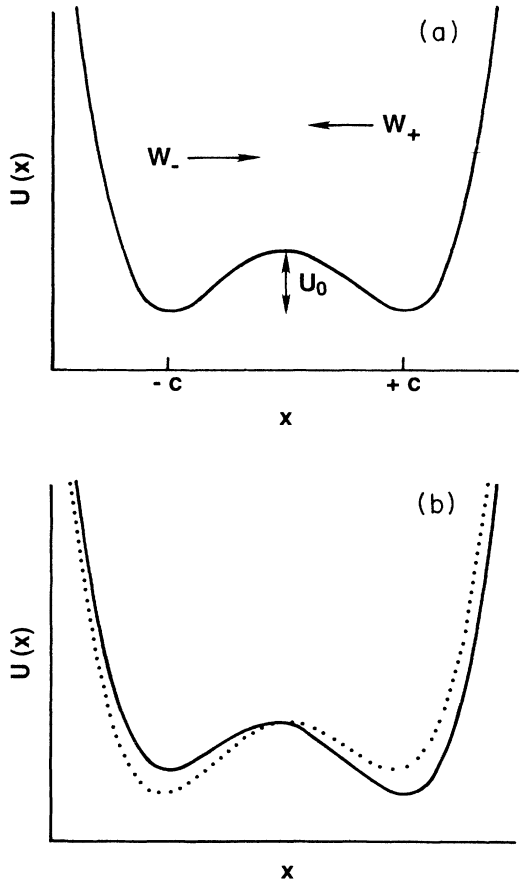

FIG. 2. (a) Quartic potential minima at $\pm c$, barrier height U_0, and escape rates $W_\pm$ out of the $\pm$ wells. (b) Sinusoidally modulated potential at two times 180° out of phase.

The position of the particle $x(t)$ is considered to be the output of the system, and we choose to focus on the power spectrum $S(\Omega)$, where $S(\Omega)=|X(\Omega)|^2$, and $X(\Omega)$ is the Fourier transform of $x(t)$. $S(\Omega)$ has a (nearly) Lorentzian shape $S(\Omega)\sim 2\alpha/(\alpha^2+\Omega^2)$ as is typical for many noise-driven systems, linear or not, in which some shortest time scale or fastest rate α is imposed on the motion x. Though the input noise power may be flat out to some very high frequency, the output is roughly flat out to $\Omega\approx\alpha$, and then falls off like $S(\Omega)\sim\Omega^{-2}$ for still higher frequencies.

On top of this picture we add a periodic signal which has the effect of tilting the potential first to the right, so a particle is more likely to be near $+c$, and then to the left one-half cycle later [see Fig. 2(b)]. Throughout this paper, we presume that the signal amplitude is small enough that, in the absence of any noise, it is insufficient to force a particle to move from one well to the other. In a sense to be quantified later, it is also assumed that the signal period is longer than some characteristic intrawell relaxation time for the system. The periodic signal has the effect of modulating the transition rate, making $W_+(t)$, the rate out of the + well, oscillate out of phase with $W_-(t)$, the rate out of the − well. For very small noise, these rates are still too slow for there to be appreciable hopping and the small periodic modulation remains unimportant.

As we will show, the characteristic rate associated with this bistable system is given by $\alpha=W_++W_-$. As D is increased from a very low value, both W_+ and W_- increase, and therefore α increases. As we may expect from the Lorentzian shape of the output noise spectrum, the output noise power (at the signal frequency ω_s) $N=S_{\text{noise}}(\Omega\approx\omega_s)$ increases until $\alpha\approx\omega_s$. What is surprising is that the signal output power $S=S_{\text{signal}}(\omega_s)$, also grows and even faster than N. There is a cooperative phenomenon taking place: Incoherent noise power is feeding into the coherent output signal. At one extreme of the cycle, it becomes likely for a particle in the − well to jump to the + well; half a cycle later it is likely to jump back. These relatively large excursions in the particle's position show up as an output with a strong periodic component to it and an enhanced spike in the output spectrum at the signal frequency. With too much noise, though, the jumps may occur over a whole range of times during each half cycle, and the coherence becomes lost. The cooperation subsides, and the noise in feeds the noise out, not the signal out.

This is the essence of the physical mechanism behind stochastic resonance in what we shall call the low signal frequency regime. It should be pointed out that the SNR does not, in fact, attain its maximum at the same value of D for which S is at its peak. The SNR continues to increase after S begins to decline because for a time the noise N, which has also peaked, decreases faster than does the signal. Thus the SNR ratio actually continues to increase until eventually S starts to decrease more rapidly

than N. The SNR then falls off gradually as $D \to \infty$. Later we will discuss another regime, in which the signal frequency is relatively high, which is quite similar in many respects. There is a slight difference in the cooperative mechanism, but the value of D at which the SNR is a maximum is very nearly independent of the signal frequency in both regimes.

A natural simplification of the double-well problem is the discrete two-state system. (As a model for quantum systems, it is of interest in its own right.) The two-state system with random hopping between states but no periodic modulation gives rise to so-called telegraph noise. It is a straightforward calculation to find that the power spectrum of such a system is a simple Lorentzian. The analysis assumes two hopping rates, one in each direction, but how in a real physical system the external noise actually determines these rates is left unspecified. Eckmann and Thomas studied a two-state system for which the hopping rates had a small periodic modulation added, one rate 180° out of phase with the other.[8] Their conclusion was that sweeping through different ω_s did not give rise to a peak in the output signal. We confirm here that there is only a monotonic decrease in the signal and SNR ratio with increasing ω_s. Because they made no attempt to present a relationship between input noise D and the hopping rates $W_\pm$, they could not study the more central issue of output power as a function of D. In Sec. VI the rates $W_\pm(D)$ are derived for the Schmitt trigger circuit which is very nearly a two-state system, and we show how their behavior yields stochastic resonance.

We conclude this section with a short list of the main issues to be addressed. Foremost is to find expressions for signal and noise output from bistable systems which agree with simulations and give added insight into the physical source of this phenomenon. From these expressions we can also make some helpful predictions regarding stochastic resonance. The primary prediction is the value of input noise at which the SNR will be enhanced. In addition, one can use equations for S and N to help adjust the other system parameters to make the effect more pronounced or to make it occur within the constraints of a physically realizable experiment. In particular, the effect of the choice of signal frequency can be examined. Finally, by breaking the problem into a general theory and a specific calculation of the transition rate for a particular system of interest, one can better see the necessary features present in all systems displaying stochastic resonance as well as the differences between individual systems.

III. GENERAL THEORY

In this section we derive expressions for the signal and noise power from a bistable system, in a way which is independent of the precise dynamics of the system. To make these results useful for a particular system, one must have an expression for the transition rate or hopping rate as a function of the input noise and other parameters. Such rates are derived from the details of the system dynamics; in this section the rate is assumed known. *Typically, this expression for the transition rate will be valid only in the adiabatic limit,* when the signal frequency is much slower than some relaxation time τ_r^{-1}. For the double-well system, for example, τ_r is the time for probability *within* one well to equilibrate.

In the approach used below the dynamical variable is taken to be discrete: either x_- or x_+ with probabilities $n_\pm = \text{prob}(x = x_\pm)$. If the true dynamics are continuous, as with the double well, then we define

$$n_- = 1 - n_+ = \int_{-\infty}^{x'} p(x)dx \ , \tag{3.1}$$

where x' is the location of the potential maximum separating the two wells. In general, the modulation of the potential will cause the positions of the potential minima and maximum to oscillate, and depending on the level of approximation used, it may be necessary to take this into account. The governing rate equation, then, is just

$$\frac{dn_+}{dt} = -\frac{dn_-}{dt} = W_-(t)n_- - W_+(t)n_+ = W_-(t) - [W_-(t) + W_+(t)]n_+ \ , \tag{3.2}$$

where $W_\pm(t)$ is the transition rate *out of* the $\pm$ state. Note that $W_\pm(t)$ is time periodic due to the periodic signal.

The reduction from a continuous bistable system whose probability evolves according to a Fokker-Planck equation to a discrete system governed by a rate equation has been carried out formally,[15] and the extension to a periodically modulated system is straightforward.[13] For the purpose of computing moments, the probability density is effectively

$$p(x,t) = n_+(t)\delta(x - x_+) + n_-(t)\delta(x - x_-) \ . \tag{3.3}$$

Values for $x_\pm$ can be chosen to minimize the error in this reduction. For simplicity it will be assumed that the system is symmetrical about $x = 0$ so that $x_+ = -x_- = c$ and the value for c is chosen to minimize the error in the variance of x. The variance for an unmodulated two-state system in its steady state ($n_+ = n_- = \frac{1}{2}$) is just

$$\langle x^2 \rangle = \int_{-\infty}^{\infty} x^2 p(x)dx = x_+^2 n_+ + x_-^2 n_- = c^2 \ . \tag{3.4}$$

The solution to the linear first-order differential equation with periodic coefficients Eq. (3.2) is given by

$$n_+(t) = g^{-1}(t)\left[n_+(t_0)g(t_0) + \int_{t_0}^{t} W_-(t')g(t')dt'\right] \ ,$$
$$g(t) = \exp\left[\int^t [W_+(t') + W_-(t')]dt'\right] \ . \tag{3.5}$$

In general, the form of $W_\pm$ will be such that Eq. (3.5) cannot be integrated in terms of known functions. We assume, though, that the rate is of the form

$$W_\pm(t) = f(\mu \pm \eta_0 \cos\omega_s t) \ , \tag{3.6}$$

where μ is a dimensionless parameter formed from the ra-

tio of a "potential barrier" to the noise, and η_0 is the dimensionless strength of the modulation of μ by the signal. (The standard Kramers formula is of this form with $\eta_0=0$.) Under these assumptions, we can use the following expansion in the small parameter $\eta=\eta_0\cos\omega_s t$:

$$\begin{aligned} W_{\pm}(t)&=\tfrac{1}{2}(\alpha_0\mp\alpha_1\eta_0\cos\omega_s t \\ &\quad +\alpha_2\eta_0^2\cos^2\omega_s t\mp\cdots), \\ W_+(t)+W_-(t)&=\alpha_0+\alpha_2\eta_0^2\cos^2\omega_s t+\cdots, \end{aligned} \tag{3.7}$$

where

$$\tfrac{1}{2}\alpha_0=f(\mu),\quad \tfrac{1}{2}\alpha_n=\frac{(-1)^n}{n!}\frac{d^n f}{d\eta^n}(\mu)\ . \tag{3.8}$$

The factor of $(-1)^n$ is included to keep α_1 positive (since f must be a decreasing function of its argument), and the $\frac{1}{2}$ is added for later convenience. Equation (3.5) may now be integrated to give the time-dependent probability, to first order in η,

$$n_+(t|x_0,t_0)=\frac{1}{2}\left[e^{-\alpha_0(t-t_0)}\left[2\delta_{x_0c}-1-\frac{\alpha_1\eta_0\cos(\omega_s t_0-\phi)}{(\alpha_0^2+\omega_s^2)^{1/2}}\right]+1+\frac{\alpha_1\eta_0\cos(\omega_s t-\phi)}{(\alpha_0^2+\omega_s^2)^{1/2}}\right], \tag{3.9}$$

where $\phi=\tan^{-1}(\omega_s/\alpha_0)$. Here the Kronecker δ function δ_{x_0c} is 1 if the particle was initially in the + state and 0 if it was in the − state at $t=t_0$. The quantity $n_+(t|x_0,t_0)$ is the conditional probability that $x(t)$ is in the + state at time t, given that the state at time t_0 was x_0 (which may be $+c$ or $-c$). Retaining higher powers of η in Eq. (3.5) leads to higher harmonics in Eq. (3.9), which in turn generates higher harmonics in the observed power spectrum.

From Eq. (3.9), any desired statistical information can be computed. Of particular interest is the autocorrelation function, which is given by the four terms

$$\begin{aligned} \langle x(t)x(t+\tau)|x_0,t_0\rangle &= +c^2n_+(t+\tau|+c,t)n_+(t|x_0,t_0)-c^2n_+(t+\tau|-c,t)n_-(t|x_0,t_0) \\ &\quad -c^2n_-(t+\tau|+c,t)n_+(t|x_0,t_0)+c^2n_-(t+\tau|-c,t)n_-(t|x_0,t_0) \\ &= c^2\{[2n_+(t+\tau|+c,t)-1+2n_+(t+\tau|-c,t)-1]n_+(t|x_0,t_0)-[2n_+(t+\tau|-c,t)-1]\}\ . \end{aligned} \tag{3.10}$$

For example, the term $+c^2n_+(t+\tau|-c,t)n_-(t|x_0,t_0)$ represents the case that at t_0 the particle is at x_0, at t it is at $-c$, and at $t+\tau$ it is at $+c$. This greatly simplifies in the limit $t_0\to-\infty$; the autocorrelation function is then just

$$\begin{aligned} \langle x(t)x(t+\tau)\rangle &= \lim_{t_0\to-\infty}\langle x(t)x(t+\tau)|x_0,t_0\rangle \\ &= c^2e^{-\alpha_0|\tau|}\left[1-\frac{\alpha_1^2\eta_0^2\cos^2(\omega_s t-\phi)}{\alpha_0^2+\omega_s^2}\right]+\frac{c^2\alpha_1^2\eta_0^2\{\cos\omega_s\tau+\cos[\omega_s(2t+\tau)+2\phi]\}}{2(\alpha_0^2+\omega_s^2)}\ . \end{aligned} \tag{3.11}$$

Notice that the power spectrum, which is the Fourier transform of the autocorrelation function, is a function of t as well as Ω. In an experiment t represents the time at which one begins to take data. Typically one takes an ensemble of many time series at times $t_1,t_2,\ldots$, computes the power spectrum for each one, and averages them together. Unless for some reason the experimenter has taken care to synchronize the phases $(\omega_s t_1-\phi),(\omega_s t_2-\phi),\ldots$, the values of t must properly be treated as a random variable, uniformly distributed over 0 to $2\pi/\omega_s$. To account for this averaging of power spectra taken at random times, one must average the power spectrum over t:

$$\langle S(\Omega)\rangle_t=\frac{\omega_s}{2\pi}\int_0^{2\pi/\omega_s}S(\Omega,t)dt\ .$$

Because this averaging and the Fourier transform commute, we choose to perform the averaging first, on the autocorrelation function:

$$\langle\langle x(t)x(t+\tau)\rangle\rangle_t=\frac{\omega_s}{2\pi}\int_0^{2\pi/\omega_s}\langle x(t)x(t+\tau)\rangle dt=c^2e^{-\alpha_0|\tau|}\left[1-\frac{\alpha_1^2\eta_0^2}{2(\alpha_0^2+\omega_s^2)}\right]+\frac{c^2\alpha_1^2\eta_0^2\cos\omega_s\tau}{2(\alpha_0^2+\omega_s^2)}\ . \tag{3.12}$$

Finally, the power spectrum is given by

$$\begin{aligned} \langle S(\Omega)\rangle_t &= \int_{-\infty}^{\infty}\langle\langle x(t)x(t+\tau)\rangle\rangle_t e^{-i\Omega\tau}d\tau \\ &= \left[1-\frac{\alpha_1^2\eta_0^2}{2(\alpha_0^2+\omega_s^2)}\right]\left[\frac{2c^2\alpha_0}{\alpha_0^2+\Omega^2}\right]+\frac{\pi c^2\alpha_1^2\eta_0^2}{2(\alpha_0^2+\omega_s^2)}[\delta(\Omega-\omega_s)+\delta(\Omega+\omega_s)]\ . \end{aligned} \tag{3.13}$$

From this point on we will use $S(\Omega)$ to denote the *one-sided* t-averaged power spectrum [$S(\Omega)$ defined for Ω positive only[16]],

$$S(\Omega)=\langle S(\Omega)\rangle_t+\langle S(-\Omega)\rangle_t=\left[1-\frac{\alpha_1^2\eta_0^2}{2(\alpha_0^2+\omega_s^2)}\right]\left[\frac{4c^2\alpha_0}{\alpha_0^2+\Omega^2}\right]+\frac{\pi c^2\alpha_1^2\eta_0^2}{\alpha_0^2+\omega_s^2}\delta(\Omega-\omega_s)\ . \tag{3.14}$$

This is the basic result of this section. Notice that the spectrum divides naturally into two parts: the signal output which is a δ function at the signal frequency, and the broadband noise output, which is a Lorentzian bump centered at $\Omega=0$. The noise spectrum is the product of the Lorentzian obtained with no signal $\eta_0=0$ and a correction factor which represents the effect of the signal on the noise. For sufficiently small-signal amplitude, this factor is nearly unity. The correction factor has the effect of an overall reduction of the noise power, and this reduction of the noise is most pronounced when the signal is of low frequency $\omega_s \ll \alpha_0$ and large amplitude. The effect of the signal is to transfer power from the broadband into the δ function spike. The total output power, signal plus noise, is independent of the signal amplitude and frequency. This can be understood as a consequence of Parseval's relation—the time integral of the square of the signal is equal to the integral of the power spectrum over all frequencies—and the fact that the system takes on the discrete values $\pm c$ at all times. Since the integral over a time T of the square of the signal must always be the constant Tc^2, the total power must be a constant as well. For continuous systems, such as the double well, the two-state model used here is only an approximation, and as such it may be expected that the total power for these systems will not be conserved exactly.

IV. ON THE COMPARISON OF THE THEORY WITH EXPERIMENTS

In this section we take time out to make a few remarks concerning the comparison of the general theory with both numerical simulations and laboratory experiments. To demonstrate that Eq. (3.14) correctly predicts the signal and noise power we can create a simple system for which the transition rate between two states is given precisely by

$$W_{\pm}=\tfrac{1}{2}(\alpha_0\pm\alpha_1\eta_0\cos\omega_s t)\ .$$

That is, we let α_0 and $\alpha_1\eta_0$ be parameters of the system, directly rather than as terms in an expansion of a function which is already an approximation. On a digital computer, at each timestep a random number ξ is chosen uniformly on the interval 0 to 1. If the system is currently in the $\pm$ state ($x=\pm c$), ξ is compared with

$$p_{\pm}(t)=\Delta t W_{\pm}(t)=\frac{\Delta t}{2}(\alpha_0\pm\alpha_1\eta_0\cos\omega_s t)\ , \tag{4.1}$$

where Δt is the timestep. If $\xi<p_{\pm}$, the system is changed to the other state. During any finite timestep, the continuous time system of Eq. (3.2) is capable of making two or more transitions, a situation not accounted for by this discrete time scheme. Since the probability of making n transitions in a time Δt is $(1/n!)p_{\pm}^n e^{-p_{\pm}}$, the probability that such multiple transitions will occur can be held to less than q by making

$$\Delta t<2\sqrt{2q}\ /(\alpha_0+\alpha_1\eta_0)\ .$$

In practice, the timestep can be systematically decreased until further reduction no longer has an appreciable effect on the spectrum.

Typically, the time series data must be windowed in order to reduce the effects of having a time series of finite length. That is, the elements of the time series are weighted by coefficients chosen to deemphasize the start and end of the series, while keeping the total power a constant. From the windowed data the power spectrum is computed with a fast Fourier transform. To reduce the variance within each frequency bin, a large ensemble of such spectra should be averaged together. In this work we plot the power spectral density (PSD), the total power in each frequency bin divided by the size of one bin [the bandwidth (Δ)], because the plot is then independent of the choice of the total sampling time (the reciprocal of the bandwidth).

Figure 3 is a plot of the power spectral density as a function of frequency from a simulation of Eq. (3.2) with the transition rate computed according to Eq. (4.1). There is excellent agreement with the theory of Eq. (3.14). For N, the noise at the signal frequency, we use an interpolated average of the PSD from neighboring frequency bins. The natural measure for the signal from such a spectrum is the PSD in the bin corresponding to the signal frequency. There are several complications in comparing this "experimental signal," S_{expt}, with the theoretical expression for the signal in Eq. (3.14). First, the process of windowing before Fourier analyzing the time series has an effect on coherent signals which does not apply to random noise: Signal peaks are reduced by a factor called the processing gain.[17] The processing gain G is given by

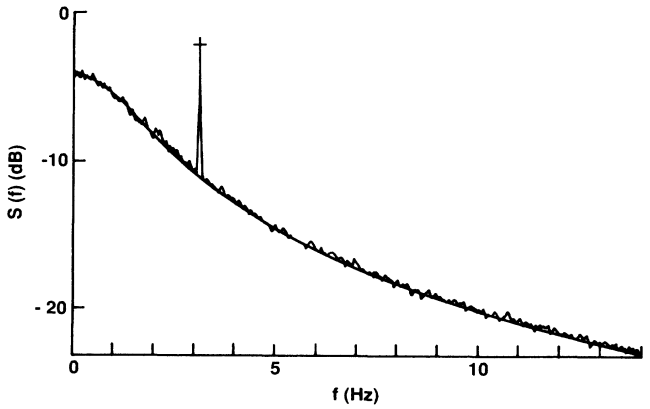

FIG. 3. Typical power spectrum $S(f)$ from the simple system of Sec. IV with $f_s=3.125$, $\alpha_0=10$, $\alpha_1\eta_0=5$, and $\Delta t=0.005$. The cross indicates the location of the signal power S_{expt} given by the theory.

$$G=\frac{\left[\sum_i w_i\right]^2}{\sum_i (w_i)^2}\ , \tag{4.2}$$

where w_i is the window coefficient multiplying the ith sample in the time series. G is typically between 1 (for no windowing) and 0.5. Next, one must take into account the fact that the total power in the frequency bin includes the integrated PSD of the noise which is also present in that bin. A third complication arises from the fact that while the units for the noise term in Eq. (3.14) are power spectral density (power per unit bandwidth), the signal term is the product of a δ function (with units of bandwidth^{-1}) and the total power under the δ function. Because the experimentally measured signal S_{expt} is a PSD, the total theoretical signal power must be divided by the bandwidth Δ. (Still another complication—"scalloping loss," causing signal power to be divided among several bins—can be avoided in simulations by setting the signal frequency to be centered on one of the bins.) Thus we have the expression

$$S_{\text{expt}}=(SG+N\Delta)/\Delta\ , \tag{4.3}$$

where S and N are taken from Eq. (3.14). In general, in experiments it is more convenient to compute the power spectrum in terms of the frequency f rather than the circular frequency Ω so the δ function $\delta(\omega_s-\Omega)=\delta(f_s-f)/2\pi$ introduces a factor of $(2\pi)^{-1}$ into the expression for S. Notice from Eq. (4.3) that the smallest possible value for the experimental signal-to-noise ratio (R_{expt})

$$R_{\text{expt}}=(SG/\Delta+N)/N \tag{4.4}$$

is one, not zero.

By varying one parameter while holding the others fixed, one may take a series of power spectra like Fig. 3, measure the signal and noise power at each parameter setting, and then plot the results. In Figs. 4–6 the experimental signal, noise, and signal-to-noise ratio are plotted as a function of three parameters. Holding the input signal fixed and varying α_0 (which may be though of as a reciprocal "barrier height"), from Eq. (3.14) the noise may be expected to peak at roughly $\alpha_0=\omega_s$, and the signal should have a nearly Lorentzian profile with a "knee" (that is, its 3-dB point) at ω_s. In Fig. 4(a) the signal and noise are shown as a function of α_0, with ω_s held fixed, and there is good agreement with the theory. Figure 4(b) presents R_{expt} as a function of α_0, also with good agreement. The effect of varying the signal amplitude, represented by the $\alpha_1\eta_0$ term, is shown in Fig. 5. From Eq. (3.14), one may expect the output signal power to increase with $(\alpha_1\eta_0)^2$ and the noise to similarly decrease, and these predictions are confirmed. The signal has a Lorentzian profile in the signal frequency ω_s, with a knee at $\omega_s=\alpha_0$. The noise has approximately the same ω_s dependence, but also has the small correction factor discussed in Sec. III. Figure 6(a) shows the effect of ω_s on signal and noise and their 3-dB points agree nicely with $f_{3\text{-dB}}=\alpha_0/2\pi=1.6$. The signal-to-noise ratio is nearly independent of ω_s [Fig. 6(b)].

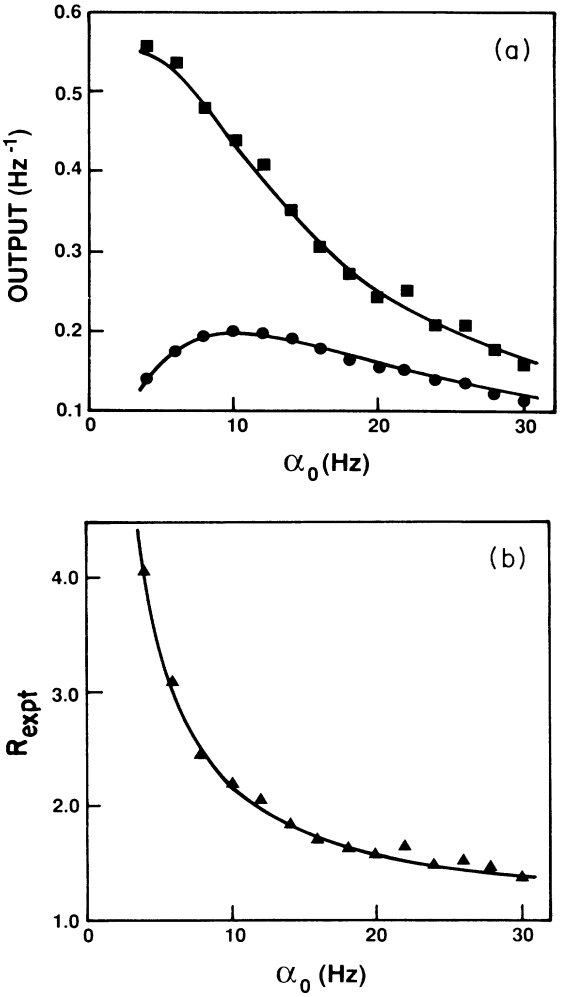

FIG. 4. (a) Output power spectral density for signal (squares) and noise (circles) as a function of reciprocal "barrier height" α_0 ($\omega_s=9.8$, $\alpha_1\eta_0=3$, and $\Delta t=0.005$). (b) Signal-to-noise ratio R_{expt} as a function of α_0 with the same parameters.

V. THE DOUBLE-WELL SYSTEM

The quartic potential system (Fig. 2) is of particular interest because it represents the simplest bistable system in a continuous variable. In the presence of a modulating signal, this potential has the form

$$U(x,t)=-\frac{a}{2}x^2+\frac{b}{4}x^4-\epsilon x\cos\omega_s t\ , \tag{5.1}$$

where ϵ and ω_s are the signal amplitude and frequency. This may also be written

$$U(x,t)=U_0\left[-2\left[\frac{x}{c}\right]^2+\left[\frac{x}{c}\right]^4\right]-U_1\left[\frac{x}{c}\right]\cos\omega_s t\ , \tag{5.2}$$

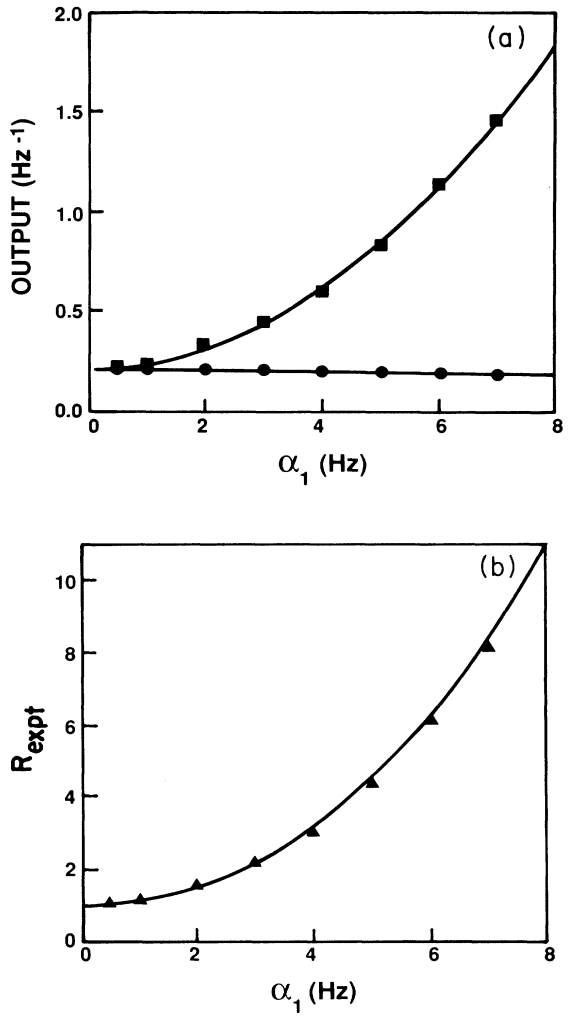

FIG. 5. (a) Output power spectral density for signal (squares) and noise (circles) as a function of signal amplitude $\alpha_1\eta_0$ ($f_s=3.125$, $\alpha_0=10$, and $\Delta t=0.005$). (b) Signal-to-noise ratio R_{expt} as a function of $\alpha_1\eta_0$ with the same parameters.

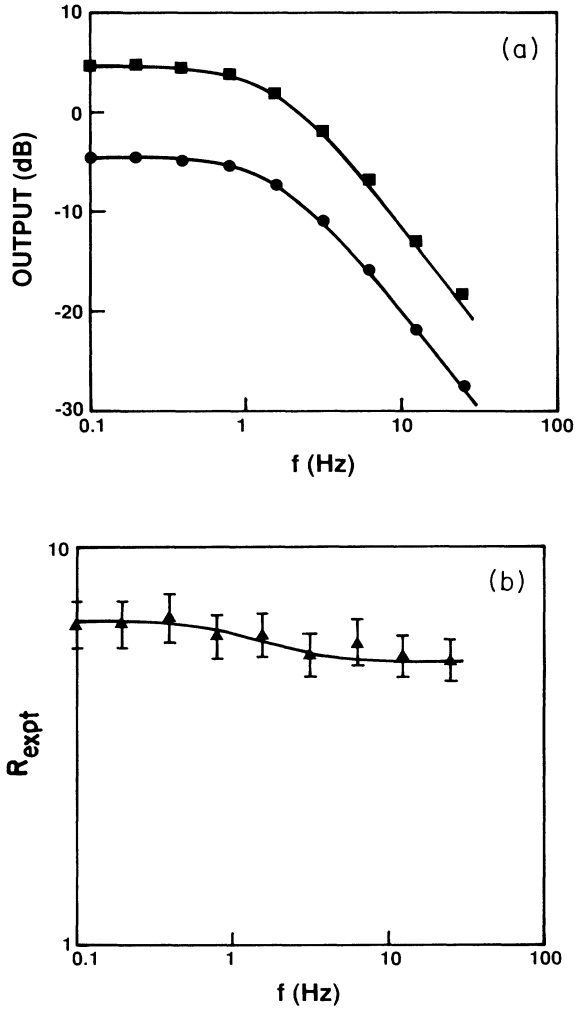

FIG. 6. (a) Output power spectral density for signal (squares) and noise (circles) as a function of signal frequency f_s ($\alpha_0=10$, $\alpha_1\eta_0=5$, and $\Delta t=0.005$). (b) Signal-to-noise ratio R_{expt} (linear scale) as a function of f_s with the same parameters.

where the potential minima are at $\pm c=\pm\sqrt{a/b}$ when $\epsilon=0$, $U_0=a^2/4b$ is the $\epsilon=0$ barrier height, and $U_1=\epsilon c$ is the amplitude of modulation in the barrier height. In the limit of large damping, the equation of motion for a randomly forced particle is

$$\dot{x}=-\partial_x U(x,t)+\sqrt{D}\,\xi(t)\ . \tag{5.3}$$

Here $\xi(t)$ represents Gaussian distributed white noise, such that $\langle\xi(t)\rangle=0$ and $\langle\xi(t)\xi(t+\tau)\rangle=\delta(\tau)$, and D is the variance of the noise.

In the absence of modulation ($\epsilon=0$) the mean first passage time is given by the Kramers time

$$\tau_K=W_K^{-1}=\frac{2\pi e^{2U_0/D}}{[|U''(0)|U''(c)]^{1/2}}=\frac{\sqrt{2}\pi}{a}e^{2U_0/D}\ . \tag{5.4}$$

Because the expression for the Kramers transition rate depends only on the potential barrier height and the curvature of the potential at the maximum and minima, it is not especially important that the potential is precisely Eq. (5.1), i.e., the results carry over directly to a wide variety of similar systems. The Kramers rate formula is derived under the assumption that the probability density *within* a well is roughly at equilibrium, a Gaussian distribution centered about the minimum. Thus in order to use the modified Kramers rate,

$$W_{\pm}(t)=\frac{a}{\sqrt{2}\pi}\exp[-2(U_0\pm U_1\cos\omega_s t)/D]\ , \tag{5.5}$$

the signal frequency must be much slower than the characteristic rate for probability to equilibrate within a well. This rate is just the curvature at the well minimum $U''(\pm c)$. Thus the adiabatic approximation is valid only for $\omega_s\ll U''(\pm c)=2a$.

For the purpose of applying the results of Sec. III to

the double-well problem, the coefficients α_0 and α_1 in the expansion for $W_{\pm}(t)$ must be computed from Eq. (3.8). Comparing Eqs. (3.6) and (5.5) we have $\mu = U_0/D$, $\eta_0 = U_1/D = \epsilon c/D$, so that

$$f(\mu+\eta_0\cos\omega_s t)=\frac{a}{\sqrt{2\pi}}e^{-2(\mu+\eta_0\cos\omega_s t)},$$
$$\alpha_0 = 2f(\eta=0)=\frac{\sqrt{2}a}{\pi}e^{-2U_0/D}, \tag{5.6}$$
$$\alpha_1 = -2\frac{df}{d\eta}(\eta=0)=\frac{2\sqrt{2}a}{\pi}e^{-2U_0/D}=2\alpha_0 .$$

The expressions for α_0 and α_1 may be substituted into Eq. (3.14) for the power spectrum,

$$S(\Omega)=\left[1-\frac{\frac{4a^2\epsilon^2c^2}{\pi^2D^2}e^{-4U_0/D}}{\frac{2a^2}{\pi^2}e^{-4U_0/D}+\omega_s^2}\right]\left[\frac{\frac{4\sqrt{2}ac^2}{\pi}e^{-2U_0/D}}{\frac{2a^2}{\pi^2}e^{-4U_0/D}+\Omega^2}\right]$$
$$+\left[\frac{\frac{8a^2\epsilon^2c^4}{\pi D^2}e^{-4U_0/D}}{\frac{2a^2}{\pi^2}e^{-4U_0/D}+\omega_s^2}\right]\delta(\Omega-\omega_s), \tag{5.7}$$

and the signal-to-noise ratio (R)

$$R=\left[\frac{\sqrt{2}a\epsilon^2c^2}{D^2}e^{-2U_0/D}\right]\times\left[1-\frac{\frac{4a^2\epsilon^2c^2}{\pi^2D^2}e^{-4U_0/D)}}{\frac{2a^2}{\pi^2}e^{-4U_0/D}+\omega_s^2}\right]^{-1}. \tag{5.8}$$

Notice that the second factor in Eq. (5.8) represents the fraction of the total power that is in the broadband noisy part of the spectrum. The part which is subtracted from 1 is the fraction which is in the coherent signal output. In general, the signal has only a small fraction of the total power, so the signal-to-noise ratio is approximately

$$R\approx\frac{\sqrt{2}a\epsilon^2c^2}{D^2}e^{-2U_0/D}. \tag{5.9}$$

For D very small compared to U_0, $e^{-2U_0/D}$ falls to zero more rapidly than D^2 in the denominator so $R\to 0$. At very large values of D (for which the approximations yielding the Kramers rate are no longer valid), $e^{-2U_0/D}$ approaches 1 but the D^2 in the denominator again forces $R\to 0$. In between there is a maximum value for the SNR which, from the approximate expression (5.9), may be expected at $D_{\max}\approx U_0$.

The effect of increasing the input signal power $\epsilon^2/2$ is straightforward: The signal output power increases in direct proportion and the output noise decreases very slightly. The implications of varying the signal frequency are more complicated. To examine this, in Fig. 7 we present the signal, noise, and SNR, as computed from Eqs. (5.7) and (5.8), as a function of input noise at different signal frequencies. For convenience, ω_s is normalized by the hopping rate at $D=U_0$, near which stochastic resonance is expected to peak,

$$\tilde{\omega}=\frac{\omega_s}{W(D=U_0)}=\frac{\sqrt{2\pi}\omega_s e^2}{a}.$$

In Fig. 7(a) the dotted line represents the curve of maximum values for the signal power, and is given by the relation

$$\tilde{\omega}^2=\frac{De^{-4(U_0-D)/D}}{2U_0-D},$$
$$S=c^2\eta_0^2\left[\frac{2U_0-D}{U_0}\right],$$

obtained by maximizing the expression for S, the factor multiplying the δ function in Eq. (5.7), with respect to D. The dashed curve represents the values of S when the signal frequency precisely matches the rate coefficient, $\omega_s=\alpha_0(D)=2W(D)$, i.e., $\tilde{\omega}=2e^{-2(U_0-D)/D}$. This matching was the condition for stochastic resonance heuristically derived by Benzi *et al.* It is clear that in the low-frequency regime, for which $\tilde{\omega}<1$, their condition agrees reasonably well with the theory presented here for the maximum in the signal power. In the high-frequency regime, $\tilde{\omega}>1$, the signal power shows only a broad maximum independent of $\tilde{\omega}$ at the value of D for which the signal's numerator is maximum, at $D=2U_0$. For all frequencies the signal output falls off as $\tilde{\omega}$ is increased.

The clear distinction between a low-frequency and a high-frequency regime begs the question of whether one should associate a different physical picture of stochastic resonance in these two regimes. When the signal frequency is low, the probability $p(x,t)$ has time to approach a *global* equilibrium only if $\alpha_0(D)\gtrsim\omega_s$—the particle has a high likelihood of hopping from the upper well to the lower well during the half cycle available to do so. However with larger noise, $\alpha_0(D)\gg\omega_s$, there is a substantial probability of hopping back to the upper well for a time, destroying the phasing of the transitions caused by the signal. Therefore we can say that the word "resonance" in the term stochastic resonance, while perhaps somewhat misleading, probably derives from the matching of the rates α_0 and ω_s to maximize signal power at low frequencies. For $\tilde{\omega}>1$, the principle feature is an overall decline in the signal power because fewer and fewer particles find the time to hop to the lower well during each half cycle. Increasing D helps by increasing the transition rate, but past $D=2U_0$ the increased chances of being kicked in the antiphase direction causes a gradual decline in the signal output. Thus, in the high frequency regime, the maximum in the SNR may be thought of more as a compromise than a resonance.

The power spectrum of the noise output, when the input signal is turned off, is a Lorentzian $N\sim 2\alpha_0/(\alpha_0^2+\Omega^2)$, whose width α_0 depends on D. In Fig. 7(b),

plotted in the manner of Fig. 7(a), $\tilde{\omega}=\Omega/W(D)$ is viewed as a parameter and the D dependence is emphasized. Here there is less of a distinction between low and high-frequency regimes—it is always the case that N is a maximum when $\alpha_0(D)=\Omega$. However, the peak is narrow and high for $\tilde{\omega}<1$ and broad and low for $\tilde{\omega}>1$. Figure 7(c) shows the effect on the noise of adding a signal of moderate amplitude. Though in general the effect is negligible, the theory predicts that for $\tilde{\omega}\ll 1$ there is the possibility of a small range of D for which a substantial amount of noise power is fed into the signal, causing a sharp minimum in N—the factor subtracted from 1 in the noise term is no longer small. When this term is of order 1, the small signal approximation used to derive the result is no longer valid. Because in theory this could cause the noise power to become negative (clearly unphysical), one must remain skeptical of this noise dip until it is verified experimentally. In their experiments with a Schmitt trigger circuit, Fauve and Heslot report results in which "the noise is almost suppressed," which may be an example of this phenomenon.[4] (Since this effect is a result of the general theory, it may be expected in systems as different as the Schmitt trigger and the double well.)

Finally the theoretical signal-to-noise ratio given in Eq. (5.8) is shown in Fig. 7(d). Only two values of $\tilde{\omega}$ are plotted; for all intermediate values of $\tilde{\omega}$ the curves fall in between the two shown. The interesting point here is that there is so little variation in the location or value of the SNR peak over a very wide range in $\tilde{\omega}$, and that, in general, the SNR peak is not at the same value of D for which the signal is maximum. In the low-frequency regime the signal and noise peak at about the same value of D, but until $D=D_{\max}=U_0$, the signal falls off more slowly than the noise, causing the signal-to-noise ratio to increase until $D=D_{\max}$. Mathematically, it is this crossover in the relative rates of decrease that gives rise to the

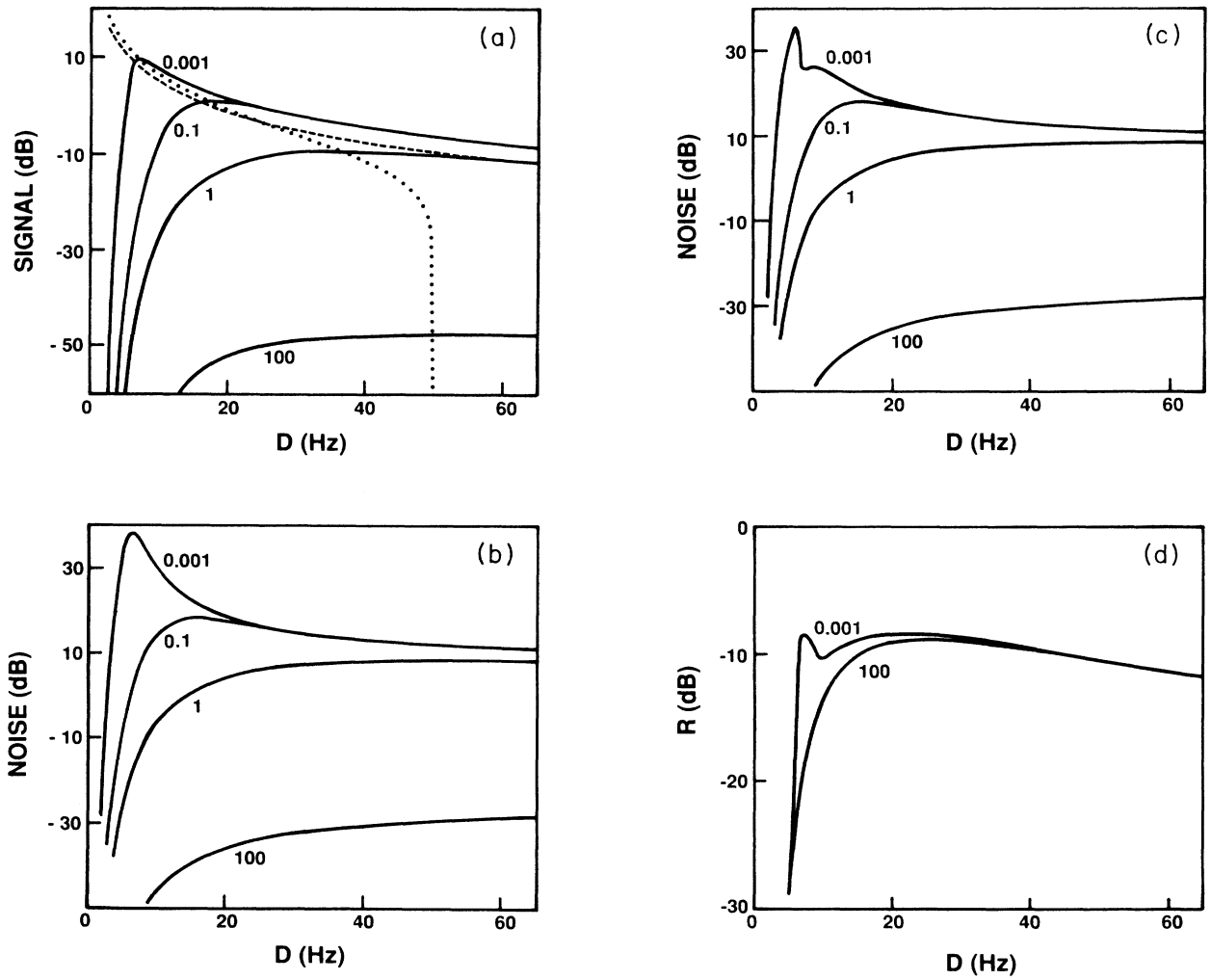

FIG. 7. (a) Theoretical output signal power as a function of input noise variance D for four different values of signal frequencies $\tilde{\omega}$. The dotted line represents the location of the signal maximum. (b) Theoretical output noise power vs D with no input signal. (c) Theoretical output noise vs D with a signal present ($\epsilon\neq 0$). (d) Theoretical signal-to-noise ratio vs D. Note the second peak present for sufficiently low $\tilde{\omega}$.

peak in the SNR, for $\tilde{\omega} < 1$. For $\tilde{\omega} > 1$, both signal and noise are still increasing at $D = D_{\max}$, but in this case there is a crossover in the rate of increase, with the noise starting to grow faster than the signal.

For the Kramers formula to apply, it was assumed that $D \ll D_0$, so there is reason to suspect that the results of Figs. 7(a)–7(d) may not be valid or may require significant correction in this regime. We turn now to simulations in order to check the range of validity of the theory. In particular, we would like to check for (1) the existence of stochastic resonance, (2) the location of $D_{\max}$, i.e., the input noise for which the SNR is largest, (3) the effect of signal amplitude and frequency on the signal and noise power, and (4) the values of the parameters, especially D, for which Eq. (5.7) reasonably predicts the output power spectrum of the system. The simulations shown below were generated by digitally integrating the equation of motion Eqs. (5.2) and (5.3) with a timestep small enough that further reducing the timestep did not appreciably alter the results. Time series data were multiplied by a Hanning window[17] and the periodgram computed using a fast Fourier transform. What is shown is the result of a large ensemble of power spectra (typically ~ 1000) averaged to reduce the expected variance.

Figure 8 presents a typical power spectrum taken from a system with $D = U_0$. The theory consistently predicts a somewhat higher output power for both noise and signal than is obtained by simulation, indicating that the simple two-state approximation used in Sec. III is not the final word for computing the power spectrum for the double well. Nevertheless, it does a reasonably good job for a fairly wide range of parameters. In particular, in comparing the signal-to-noise ratio from the theory and simulations, the overestimation tends to cancel, resulting in a surprisingly good prediction for the SNR. Evidence of this appears in Fig. 9(a), which plots the signal and noise PSD as a function of D taken from a series of spectra like those of Fig. 8. Over a substantial range of D, both S and N are overestimated by several decibels. However, in Fig. 9(b) the R_{expt} taken from the same data is off by far less. Numerous simulations have been performed over a wide range of the parameters ω_s, ϵ, and a with results similar to those in Figs. 8 and 9.[18]

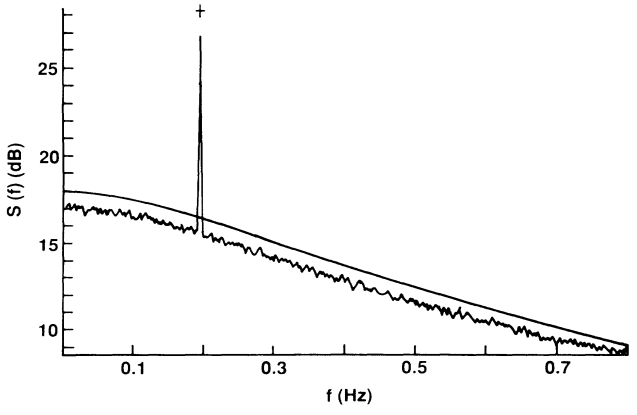

FIG. 8. Typical power spectrum $S(f)$ from the double well with $f_s = 0.195$, $a = 32$, $U_0 = 256$, $\epsilon = 8$, $D = 256$, and $\Delta t = 0.005$. Note that both the theoretical signal (cross) and noise differ from the simulation by roughly 1 dB.

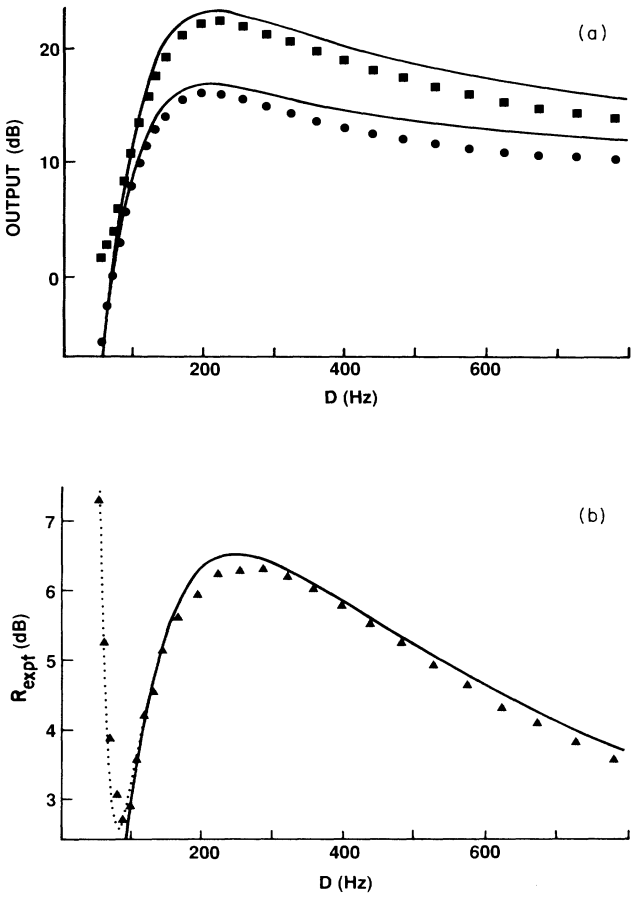

FIG. 9. (a) Output power spectral density for signal (squares) and noise (circles) as a function of input noise variance D ($f_s = 0.195$, $a = 32$, $U_0 = 256$, $\epsilon = 8$, $\Delta t = 0.005$). (b) Signal-to-noise ratio R_{expt} as a function of D with the same parameters. The dotted line represents $R_{\text{expt}_{1+2}}$, as described in the text.

Notice that for very low input noise, the limit $D \to 0$, the theory predicts that the signal-to-noise ratio should go to zero and yet it is clear from Fig. 9 that for the double well the SNR diverges. This effect can be readily understood, both on physical and theoretical levels. For very low noise, the particle makes vanishingly few hops over the barrier so that essentially all of its motion is confined within a single well. Because the theory was derived by first taking all particles within a well to be concentrated at a single point—explicitly ignoring intrawell motion—the theory derived in Sec. III cannot account for this behavior.

Instead, we can consider the motion of a particle in a single quadratic potential which is being modulated sinusoidally. Thus we expand the potential about $x = c = \sqrt{a/b}$ and drop terms which are independent of x or of order greater than 2,

$$U(y,t)=ay^2-\epsilon y\cos\omega_s t\ , \tag{5.10}$$

where $y=x-c$. The equation

$$\dot{y}=-2ay+\sqrt{D}\,\xi(t)+\epsilon\cos\omega_s t \tag{5.11}$$

can readily be solved for the autocorrelation function, one-sided power spectrum, and signal-to-noise ratio

$$\langle y(t)y(t+\tau)\rangle=\frac{D}{4a}e^{-2a|\tau|}+\frac{1}{2}\frac{\epsilon^2}{4a^2+\omega_s^2}\cos\omega_s\tau\ ,$$

$$S(\Omega)=\frac{2D}{4a^2+\Omega^2}+\frac{\pi\epsilon^2}{4a^2+\omega_s^2}\delta(\Omega-\omega_s)\ , \tag{5.12}$$

$$R=\frac{\pi\epsilon^2}{2D}\ .$$

The output SNR for the linear system is precisely equal to the input SNR and is independent of the system parameter a and the signal frequency.

There is no direct way to incorporate the expression for the single well power spectrum into a low noise theory for the double well. However, to get a rough idea, we can introduce the following ratio:

$$R_{1+2}=\frac{S_1+S_2}{N_1+N_2}\ ,$$

where $S_{1,2}$ and $N_{1,2}$ are the one- and two-well signal and noise from Eqs. (5.12) and (5.7), respectively. In fact, this gives a surprisingly good estimate for the low noise signal-to-noise ratio [see the dotted line in Fig. 9(b)], accurately predicting the values of D and SNR for the SNR minimum at which stochastic resonance "turns on." We have made no attempt to investigate further the very low noise behavior of the double well.

Since both the general theory and the Kramers rate were derived in the limit of low noise, simulations may also show important deviations from the D^{-2} falloff in the SNR predicted by Eq. (5.7). Indeed it seems somewhat fortuitous that the theory agrees so well with simulations out to at least $D\sim 3U_0$.

VI. THE TWO-STATE SYSTEM

We now turn our attention to systems in which the dynamical variable can take on only two discrete values, $\pm c$. To fix ideas we focus on a particular system, the Schmitt trigger, which is useful in digital electronics largely because its dynamics are so well modeled as a two-state system. Except during switching its output is fixed to one of two voltages to within one part in 10^4 or 10^5. Switching between states can be made to take place at rates far faster than any signal frequency of interest; this fast switching introduces complications which make the analysis of stochastic resonance of interest quite independently from the continuous variable systems. Another important feature of the Schmitt trigger is that it has hysteresis—there is a range of the input for which the circuit is bistable.

A schematic diagram of the Schmitt trigger system is presented in Fig. 10. The operational amplifier ("op amp") in the circuit behaves like a comparator: If

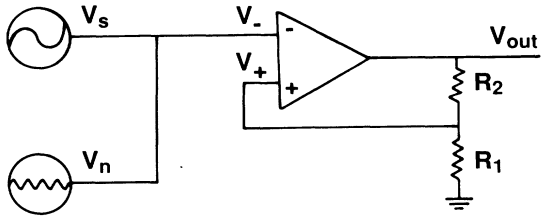

FIG. 10. Schematic diagram of the Schmitt trigger circuit driven by signal and noise.

(V_+-V_-) is positive, the output $V_{\rm out}$ is $+V_m$; if $(V_+-V_-)<0$, then $V_{\rm out}=-V_m$. For an ideal op amp, the transfer curve of Fig. 11(a) has infinite slope at $(V_+-V_-)=0$, and the time required to switch between states is zero. The transfer characteristics for the ideal op amp may be written

$$y=\mathrm{sgn}(z)\ , \tag{6.1}$$

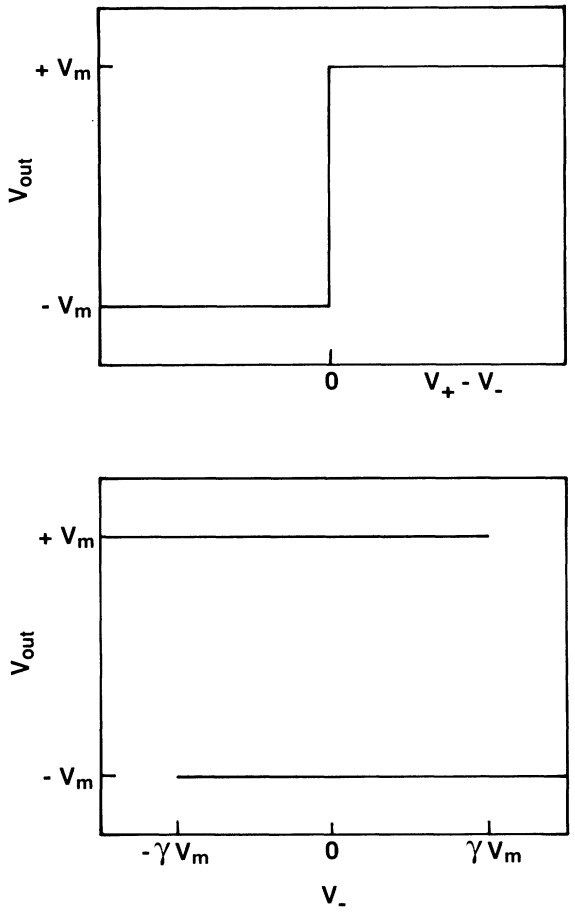

FIG. 11. (a) $V_{\rm out}$ as a function of (V_+-V_-) for an ideal operational amplifier. A real operational amplifier has a finite slope at the origin. (b) $V_{\rm out}$ as a function of V_- for an ideal Schmitt trigger.

where $y=V_{\text{out}}/V_m$, $z=(V_+-V_-)/V_m$, and $\text{sgn}(z)=+1$ if $z>0$ and $\text{sgn}(z)=-1$ if $z<0$. The positive feedback of a fraction $\gamma=R_1/(R_1+R_2)$ of the output into V_+ serves to introduce hysteresis into the system [see Fig. 11(b)].[12] Thus the ideal Schmitt trigger circuit driven by a signal and noise obeys the equation

$$\begin{aligned} y &= \text{sgn}(\gamma y-\epsilon\cos\omega_s t-x)\ , \\ x &= \sigma'\xi(t)\ , \end{aligned} \tag{6.2}$$

where $\epsilon=V_s/V_m$ is the normalized signal amplitude and $\sigma'=V_n/V_m$ is the square root of normalized noise variance.

The goal is to cast the problem in such a form that we can use the general theory from Sec. III to compute the signal and noise power. In particular, we need to compute the rates $W_{\pm}(t)$ at which the system exits the $\pm$ states. If we assume that $\xi(t)$ represents white noise with a correlation time of zero, there arises immediately a problem. For white noise, in any finite time Δt the variable $x(t)$ will take on all possible values with finite probability. This implies that the ideal Schmitt trigger with infinitesimal switching time will switch infinitely often in any time Δt and the total output power will be infinite. For this reason, we must allow either $x(t)$ to represent colored noise with a finite correlation time τ_c, or use a more realistic model for the behavior of the op amp, or both. If the switching time of the system is long compared to τ_c, it is necessary to drop the two-state model in favor of a continuous variable system but the noise may continue to be modeled as white. If the switching time is short compared to τ_c, as is the case here, only the white-noise approximation need be modified. For completeness, in what follows we introduce both of these refinements to the model but only the effect of a nonzero τ_c is ultimately used in the calculation of the transition rate and output power spectrum.

A closer approximation to the dynamics of the operational amplifier is given by

$$\dot{y}=-\beta[y-\tanh(Az)]\ , \tag{6.3}$$

where β is a relaxation rate, and A is a parameter representing the slope of the transfer curve at $z=0$. In the limit $\beta, A\to\infty$ we recover the equation for the ideal op amp, Eq. (6.1). For colored noise, we may let x be given by the output of an Ornstein-Uhlenbeck process,

$$\dot{x}=-kx+\sigma\xi(t)\ , \tag{6.4}$$

where $\xi(t)$ is again δ correlated white noise, $k=\tau_c^{-1}$, and $\sigma=\sqrt{2k}\,V_n/V_m$ so that the variance of x is $\langle x^2\rangle=\sigma^2/2k=V_n^2/V_m^2$. Hence a model for the Schmitt trigger which avoids the problem of infinite power is the two-dimensional system

$$\begin{aligned} \dot{y} &= -\beta\{y-\tanh[A(\gamma y-\epsilon\cos\omega_s t-x)]\}\ , \\ \dot{x} &= -kx+\sigma\xi(t)\ . \end{aligned} \tag{6.5}$$

In the range $-\gamma-\epsilon\cos\omega_s t<x<\gamma-\epsilon\cos\omega_s t$ the system has two stable states, which for large A are at $y\approx\pm1$. If the system is in the $+$ state, y remains fixed at very nearly $+1$ until the random variable x becomes greater than $x_+=\gamma-\epsilon\cos\omega_s t$, at which time it relaxes exponentially to $y=-1$ with a time constant β^{-1}. Similarly the system switches from the $-$ to the $+$ state when x crosses below $x_-=-\gamma-\epsilon\cos\omega_s t$.

By changing over to a continuous variable for y it may seem we have abandoned the two-state model to study the Schmitt trigger. In fact, only the use of colored noise for x was strictly necessary to make the problem tractable and give a good correspondence to a real circuit. A continuous variable y serves here to give a fuller understanding of the circuit and the reasoning behind the derivation of the transition rate.

There a number of possible routes one may take in deriving an expression for the rate $W_{\pm}(t)$ at which systems in one state make transitions to the other state. One approach is to recast the y dynamics of Eq. (6.5) as motion in the potential

$$U(y,t)=\beta\left[\tfrac{1}{2}y^2-\frac{1}{A\gamma}\ln\cosh[A(\gamma y-\epsilon\cos\omega_s t-x)]\right]\ . \tag{6.6}$$

Notice here that x does not represent a simple additive noise; rather, it enters in a more complicated parametric form, randomly altering the shape of the double-well potential. Were it possible to simply write down an effective barrier height U_0 and curvatures $U''(\pm1)$ and $U''(0)$ one could again use Kramers theory to derive the transition rate. But the fact that the noise is not additive, nor simply multiplicative, makes this a fundamentally different problem to solve, even though the observed phenomenon may in fact be identical. It should be emphasized that the Schmitt trigger system cannot be mapped onto the double-well system in any simple way, so the transition rate must be computed using a different approach.

Nevertheless, it is still possible to write down a Fokker-Planck equation for the probability $p(x,y,t)$:

$$\begin{aligned} \partial_t p = {} & \partial_y(\beta\{y-\tanh[A(\gamma y-\epsilon\cos\omega_s t-x)]\}p) \\ & +\partial_k(kxp)+\tfrac{1}{2}\sigma^2\partial^2 xp\ . \end{aligned} \tag{6.7}$$

While there is drift in both the x and y directions there is diffusion only in the x direction—transitions between states are made not by hopping over the central barrier but by diffusing out to the edge at $x_{\pm}$. The parameters β and k are the rates of relaxation in the x and y directions. In the range $\beta\gg k$, the system collapses quickly onto the upper or lower branch, $y\approx\pm1$, and the Schmitt trigger behaves most nearly as a discrete two-state system. From this point on this condition will be assumed, and we shall reduce the continuous system of Eq. (6.5) to the problem of solving for two variables p_+ and p_-, the probability that y is near $+1$ or -1. Of course, if the Schmitt trigger were not sufficiently fast, the full two-dimensional system of Eq. (6.5) could be studied as it stands.

In the regime $\beta\gg k$ one may integrate over the y variable to give the probability of being in the $+$ or $-$ state,

$$p_+(x,t)=\begin{cases}\int_{-\infty}^{\infty}p(x,y,t)dy, & x<x_-\\ \int_{y'(x)}^{\infty}p(x,y,t)dy, & x_-<x<x_+\\ 0, & x>x_+\end{cases}$$
$$p_-(x,t)=1-p_+(x,t)\ , \tag{6.8}$$

where $y'(x)$ is the curve of the unstable equilibrium separating the two wells. The equation for $p_+(x,t)$ is then

$$\partial_t p_+ = \partial_x(kxp_+)+\tfrac{1}{2}\sigma^2\partial_x^2 p_+ + \partial_t p_-(x_-)\delta(x-x_-) \tag{6.9}$$

for $x<x_+$, and $p_+=0$ for $x>x_+$. Thus p_+ behaves according to an Ornstein-Uhlenbeck process with a source at x_- and an absorbing barrier at x_+.

The rate at which probability will exit the + state may be computed as the reciprocal of the mean time for transit from x_- to x_+. There is an exact expression for the mean first passage time,[15] given by the integral

$$T(x_-\to x_+)=2\int_{x_-}^{x_+}\frac{dx}{\psi(x)}\int_{-\infty}^{x}\frac{\psi(x')}{\sigma^2}dx' \tag{6.10}$$

with

$$\psi(x)=\exp\left[-\int_{-\infty}^{x}dx'\frac{2kx'}{\sigma^2}\right]=e^{-kx^2/\sigma^2}\ .$$

Letting $u=x\sqrt{k}/\sigma$, $u_-=x_-\sqrt{k}/\sigma$, and $u_+=x_+\sqrt{k}/\sigma$, we obtain

$$W_+^{-1}\approx T(x_-\to x_+)=\frac{2\sqrt{\pi}}{k}\int_{u_-}^{u_+}du\,e^{u^2}\phi(u)\ , \tag{6.11}$$

where $\phi(u)$ is the probability integral

$$\phi(u)=\frac{1}{\sqrt{\pi}}\int_{-\infty}^{u}e^{-u^2}du\ . \tag{6.12}$$

To apply this result to the theory of Sec. III, the expansion coefficients α_0 and α_1 must be extracted from the expression for W_+. Using the notation of Sec. III, we let $\mu=\gamma\sqrt{k}/\sigma$ and $\eta_0=-\epsilon\sqrt{k}/\sigma$. With the function $f(\mu+\eta_0\cos\omega_s t)$ given by the reciprocal of $T(x_-\to x_+)$ from Eq. (6.11) we have, finally,

$$\alpha_0=\frac{k}{\sqrt{\pi}}\left[\int_{-\gamma\sqrt{k}/\sigma}^{\gamma\sqrt{k}/\sigma}du\,e^{u^2}\phi(u)\right]^{-1},$$
$$\alpha_1=\frac{k}{\sqrt{\pi}}\left[\int_{-\gamma\sqrt{k}/\sigma}^{\gamma\sqrt{k}/\sigma}du\,e^{u^2}\phi(u)\right]^{-2}e^{k\gamma^2/\sigma^2}\times[\phi(\gamma\sqrt{k}/\sigma)-\phi(-\gamma\sqrt{k}/\sigma)]\ . \tag{6.13}$$

These can now be integrated numerically and compared with simulations.

An alternative approach which may be used to find the rate at which probability $p_+(x,t)$ "leaks out" of the + state across the absorbing boundary at x_+ is the Rayleigh-Ritz variational method. Here one assumes that the boundary at x_+ is far enough from the origin that the relaxation k is much faster than the exit rate W_+. We may expect that an initial probability distribution $p(x,t_0)=\delta(x-x_-)$ will quickly spread out to roughly the Gaussian distribution $p_0(x)$ that would exist in the limit $x_+,t\to\infty$, then slowly dissipate away at a rate W_+:

$$p_+(x,t)\approx p_0(x)e^{-W_+t},$$
$$p_0(x)\approx\left[\frac{k}{\pi\sigma^2}\right]^{1/2}e^{-kx^2/\sigma^2}\ . \tag{6.14}$$

This is a first approximation to the eigenfunction expansion

$$p_+(x,t)=\sum_{n=0}^{\infty}p_n(x)e^{-\lambda_n t}\ , \tag{6.15}$$

where λ_0 is *not* 0 because in the limit $t\to\infty$, $p_+(x,t)\to 0$. Though the signal modulates the location of both x_+ and x_-, one may assume that only variations in the position of the absorbing boundary at x_+ (for exit from the + state) result in significant modulation of W_+ because a relatively fast relaxation k causes the system quickly to "forget" its initial position. As with the computation for the double-well system, it is useful to make the adiabatic approximation that the signal frequency is slow compared to the relaxation rate of the system, $\omega_s\ll k$. Thus W_+ can be calculated first for a fixed x_+, and then $x_+=\gamma-\epsilon\cos\omega_s t$ may be substituted into the result.

Given an initial trial function for the "ground-state" probability distribution $p_0(x)$, one may use the Rayleigh-Ritz technique for estimating an upper bound for the decay rate λ_0 and therefore W_+. The trial function must satisfy the boundary conditions, $p_0(-\infty)=p_0(x_+)=0$, and should possess finite first and second derivatives.[19] An example of such a trial function is

$$p_0(u)=\begin{cases}e^{-u^2}-e^{-(2u_+-u)^2}, & u\le u_+\\ 0, & u>u_+\ .\end{cases} \tag{6.16}$$

An expression for the upper bound for W_+ is then

$$W_+=\frac{\int_{-\infty}^{\infty}[\frac{1}{2}e^{u^2}(\partial_u\partial_0)^2-e^{u^2}(p_0)^2]du}{\int_{-\infty}^{\infty}\frac{1}{k}e^{u^2}(p_0)^2du}\ . \tag{6.17}$$

This may be integrated to give

$$W_+=\frac{8ku_+^2e^{8u_+^2}\phi(-3u_+)}{\phi(u_+)-2\phi(-u_+)+e^{8u_+^2}\phi(-3u_+)}\ . \tag{6.18}$$

It is revealing to examine this result for large x_+, where it becomes

$$W_+\approx\frac{4ku_+e^{-u_+^2}}{3\sqrt{\pi}}=\tfrac{4}{3}kx_+\left[\frac{k}{\pi\sigma^2}\right]^{1/2}\exp\left[\frac{-kx_+^2}{\sigma^2}\right]\ . \tag{6.19}$$

Notice the strong similarity with the Kramers formula,

with the notable difference that σ also appears in the denominator of the prefactor. This has the unphysical effect of eventually *reducing* W_+ in the large-noise limit, but this is precisely the limit for which the approximations leading to Eq. (6.19) are not valid. Retaining the full expression (6.18) avoids this problem at high σ, and we will not consider Eq. (6.19) further.

Simulations will indicate to what extent and in what range of σ one can have confidence in expression (6.18). While this is only an upper bound for W_+, because of its simplicity it may be preferred to the integral of Eq. (6.11). Finally, the expansion coefficients for the rate given in Eq. (6.18) are

$$\alpha_0=\frac{16ku_+^2e^{8u_+^2}\phi(-3u_+)}{\Xi}\ , \tag{6.20}$$

$$\alpha_1=\frac{16k}{\Xi}\left[\frac{3u_+^2e^{-u_+^2}}{\sqrt{\pi}}-2u_+(1+8u_+^2)e^{8u_+^2}\phi(-3u_+)+\frac{16u_+^3e^{16u_+^2}\phi^2(-3u_+)}{\Xi}\right]\ ,$$

where

$$\Xi=\phi(u_+)-2\phi(-u_+)+e^{8u_+^2}\phi(-3u_+)\ .$$

To check the results of this section, we have digitally simulated the two-state system

$$\begin{aligned} y&=\mathrm{sgn}(\gamma y-\epsilon\cos\omega_s t-x)\ ,\\ \dot{x}&=-kx+\sqrt{D}\,\xi(t)\ . \end{aligned} \tag{6.21}$$

Issues of choice of timestep, power spectrum estimation, and so forth were handled in a manner similar to the double-well simulations. In Fig. 12 the signal-to-noise ratio is plotted as a function of D for a typical set of parameters. The theory expressing the rate coefficients α_0 and α_1 as the integrals given in Eq. (6.13) shows fairly good agreement. The theory derived via the Rayleigh-Ritz method in Eq. (6.20) has the correct shape and location for its maximum, but is substantially high in its estimate of the SNR. [Presumably, the variational method will lead to better results if one introduces one (or several) parameters to the trial function. We have not made any systematic study along these lines; however, we point out that if one halves both α_0 and α_1 as given in Eq. (6.20), the agreement with the simulations is dramatically improved. This fact should be considered an empirical result at this stage.]

VII. CONCLUSION

This paper has introduced a general theory for stochastic resonance in bistable systems subject to both periodic and random forcing. A more detailed account of the theory can be found in Ref. 18. The theory is helpful in understanding the physical mechanism behind the phenomenon: Within a range of input noise strength,

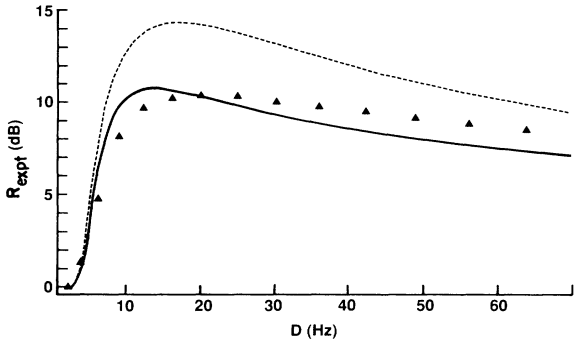

FIG. 12. Signal-to-noise ratio σ_{expt} as a function of D for the two-state system $f_s=0.781$, $\gamma=2$, $\epsilon=0.5$, $\Delta t=0.005$. The solid line represents the theory of Eq. (6.13) and the dotted line is the theory of Eq. (6.20).

there is a cooperative effect in which power in the broadband part of the spectrum is fed into the output power at the signal frequency. In the low-frequency regime, the signal power reaches a maximum when there is a matching of the signal frequency and the rate of hopping between the two states, which in turn is a function of the noise strength. Whereas the signal and noise power are functions of the signal frequency, the signal-to-noise ratio is only weakly dependent on it. However, the theory also predicts the possibility of an additional peak in the SNR at very low frequencies when there may be an extreme suppression of the noise by the signal.

The theory has been applied to the two important cases of the double-well and two-state systems. Detailed computer simulations indicate that while there are discrepancies between theory and experiment, the agreement is reasonably good. Application of the theory to other systems is straightforward, requiring only that there be an expression for the transition rate between states. Because the general theory presented in Sec. III reduces the problem to a periodically modulated telegraph process, intrawell dynamics are not accounted for, though the *ad hoc* inclusion of single-well dynamics into the theory for the double well proves to be remarkably good. While the agreement with simulation data is encouraging and there is qualitative agreement with a ring laser system, there much room for careful experiments to quantitatively verify the theory in real physical systems.

ACKNOWLEDGMENTS

We thank R. Fox, G. Nicolis, and R. Roy for stimulating discussions. One of us (B.S.M.) thanks the Physics Department at Georgia Tech for their hospitality and Mike Nauenberg and Peter Scott for continuing encouragement and support. This work was supported by a grant from the Office of Naval Research under Contract No. N00014-88-K-0494. We also acknowledge financial support from the Institute for Nonlinear Science at the University of California at Santa Cruz.

*Permanent address: Physics Board of Studies, University of California, Santa Cruz, Santa Cruz, CA 95064.

[1]R. Benzi, A. Sutera, and A. Vulpiani, J. Phys. A **14**, L453 (1981).

[2]R. Benzi, G. Parisi, A. Sutera, and A. Vulpiani, Tellus **34**, 10 (1982).

[3]R. Benzi, G. Parisi, A. Sutera, and A. Vulpiani, SIAM (Soc. Ind. Appl. Math.) J. Appl. Math. **43**, 565 (1983).

[4]S. Fauve and F. Heslot, Phys. Lett. **97A**, 5 (1983).

[5]B. McNamara, K. Wiesenfeld, and R. Roy, Phys. Rev. Lett. **60**, 2626 (1988).

[6]C. Nicolis, Tellus **34**, 1 (1982).

[7]R. Roy, R. Short, J. Durnin, and L. Mandel, Phys. Rev. Lett. **45**, 1486 (1980).

[8]J.-P. Eckmann and L. E. Thomas, J. Math. Phys. A **15**, L261 (1982).

[9]R. Benzi, A. Sutera, and A. Vulpiani, J. Phys. A **18**, 2239 (1985).

[10]R. Fox (unpublished).

[11]H. Risken, *The Fokker-Planck Equation* (Springer-Verlag, Berlin, 1984).

[12]R. Fox, G. Vemuri, and R. Roy (unpublished).

[13]B. Caroli, C. Caroli, B. Roulet, and D. Saint-James, Physica A **108**, 233 (1981).

[14]P. Byrant, K. Wiesenfeld, and B. McNamara, J. Appl. Phys. **62**, 2898 (1987).

[15]C. W. Gardiner, *Handbook of Stochastic Methods for Physics, Chemistry, and the Natural Sciences* (Springer-Verlag, Berlin, 1983).

[16]W. Press, B. Flannery, S. Teukolsky, and W. Vetterling, *Numerical Recipes in C* (Cambridge University Press, Cambridge, England, 1988).

[17]F. J. Harris, Proc. IEEE **66**, 51 (1978).

[18]Bruce S. McNamara, Ph.D. dissertation, University of California, Santa Cruz, 1988 (unpublished).

[19]S. Dattagupta and S. R. Shenoy, in *Stochastic Processes—Formalism and Applications,* edited by G. S. Agarwal and S. Dattagupta (Springer-Verlag, Berlin, 1983).